Polyhedron 208 (2021) 115415

Contents lists available at ScienceDirect

Polyhedron

journal homepage: www.elsevier.com/locate/poly

Anti-tumor effects of valproate zinc complexes on a lung cancer cell line

Emanuelle Fraga da Silva [a], Paulo Roberto dos Santos [b], Krist Helen Antunes [a], Caroline Marinho Franceschina [a], Deise Nascimento de Freitas [a], Priscila Konrad [a], Rafael Fernandes Zanin [c], Pablo Machado [d], Sidnei Moura [b], Ana Paula Duarte de Souza [a,*]

[a] Laboratory of Clinical and Experimental Immunology, Infant Center, School of Health Science, Pontifical Catholic University of Rio Grande do Sul (PUCRS), Porto Alegre, Brazil
[b] Laboratory of Natural and Synthetics Products, Biotechnology Institute, University of Caxias do Sul, Caxias do Sul, RS, Brazil
[c] Department of Health and Human Development, La Salle University, Canoas, RS, Brazil
[d] Research Center in Molecular and Functional Biology, National Institute of Science and Technology in Tuberculosis, Pontifícia Universidade Católica do Rio Grande do Sul, Porto Alegre, RS, Brazil

ARTICLE INFO

Keywords:
Cytotoxicity
Coordination compounds
Cell viability
Cell cycle
Apoptosis
SCFAs

ABSTRACT

Lung cancer is one of the most common types of cancer worldwide and the development of new treatment strategies is needed. Valproate exhibits anti-cancer properties and has been studied as a candidate for cancer therapy. Novel treatments with synthesized coordination complexes with valproate bioisosteres are promising, as they are often more effective and selective than organic molecules. We evaluated the anti-tumoral effects of two ternary complexes containing Zn^{+2}, valproate, and 2,2′-bipyridine (complex **1**) or nicotinamide (complex **2**) in a lung cancer cell line. Both complexes **1** and **2** exerted a 50% reduction in the viability of human epithelial lung cells (A549), indicating that coordination with Zn^{+2} improves the cytotoxic effects of valproate. Complex **1** increased the frequency of apoptotic cells 6-fold compared to vehicle, but it was less selective to tumor cells than complex **2**. Complex **2** reduced the frequency of cells in S phase at rates similar to valproate (from 10.2% in the control to 0% in both complex **2** and valproate). Our data highlighted the potential anti-tumoral activity of valproate-Zn^{+2} complexes and their viability as proptotypes for new drugs.

1. Introduction

Valproic acid is a short-chain fatty acid that has been used as an anti-convulsant treatment for epilepsy [1] and as a mood-stabilizing drug for the treatment of bipolar disorder [2]. Furthermore, valproate has been extensively studied as an anti-cancer agent. The anti-cancer properties of valproate are mainly attributed to its effects on cell cycle, apoptosis, cell differentiation, and DNA repair [3,4]. Different mechanisms of action have been associated with the anti-cancer effects of valproate, including inhibition of histone deacetylases (HDACs) 1 and 2 [5,6]. Aberrant expression of HDACs has been linked to several cancer types due to their role in modified the acetylation of genes involved in cell growth and promoter regions of tumor suppressor genes [7]. In a pioneer study, the anti-cancer effects of valproate were first identified and tested

Abbreviations: ^{1}HNMR, Proton Nuclear Magnetic Resonance Spectroscopy; 7-AAD, 7-Aminoactinomycin D; ^{13}CNMR, Carbon Nuclear Magnetic Resonance Spectroscopy; A549, adenocarcinoma human alveolar basal epithelial cells; Acetone D6, Deutered acetone; ATCC, American Type Culture Collection; Bipy, 2,2′-bipyridine; $CDCl_3$, Deuterated chloroform; DMEM F12, Dulbelcco's Modified Eagle's Medium; DMF, Dimethylformamide; DMSO, Dimethylsulfoxide; $\Delta\nu$COO-, Infrared variation of symmetric and asymmetric vibrations of carboxylate group; FBS, Fetal Bovine Serum; FITC, Fluorescein Isothiocyanate; FTIR, Fourier Transform Infrared Spectroscopy; HDACs, Histone Deacetylases enzymes; Hz, Hertz, NMR frequency; IC50, Half Maximal Inhibitory Concentration; $J_{H\text{-}H}$, Proton-proton spin coupling constant on NMR; MHz, Megahertz, NMR frequency; MP, Melting point; MTT, 3-(4,5-dimethylthiazol-2-yl)-2,5-diphenyltetrazolium bromide; Nic, Nicotinamide, Vitamin B3; OD, Optic density; ORTEP, Oak Ridge Thermal Ellipsoid Plot; PBS, Phosphate Buffer Saline; SD, Standard Derivation; THF, Tetrahydrofuran; UV–Vis, Ultraviolet–Visible spectrophotometry; Valp, Valproate, sodium valproate salt; Vero, *Cercopithecus aethiops* kidney normal cell line; ν_{as}, *Asymmetric vibration on infrared*; ν_s, *Symmetric vibration on infrared*; $Zn(Valp)_2Bipy$, bis-(2-propylpentanoate)2,2′-bipyridine zinc(II), complex 1; $Zn(Valp)_2(Nic)_2$, bis-(2-propylpentanoate) bis(nicotinamide) zinc(II), complex 2.

* Corresponding author at: Laboratory of Clinical and Experimental Immunology, School of Health Science, Pontifical Catholic University of Rio Grande do Sul (PUCRS), Porto Alegre, Brazil.
E-mail address: ana.duarte@pucrs.br (A.P.D. de Souza).

https://doi.org/10.1016/j.poly.2021.115415
Received 10 May 2021; Accepted 2 August 2021
Available online 8 August 2021

in neuroblastoma cells [8]. Later studies tested and confirmed the anti-tumoral effects of valproate in several different types of cancer including rectal [9], thyroid [10], cervical [11], melanoma [12], leukemia [13], and lung cancer [14,15]. A growing number of studies have started studying valproate as an adjunctive treatment for cancer in association with other chemotherapy drugs, since the anti-cancer effects valproate effects when utilized as a monotherapy are not so effective [16,17]. Conversely, strategies to improve the anti-tumor effects valproate are needed.

Lung cancer is the most common type of cancer and leading cause of death caused by cancer, representing 18% of all cancer deaths [18,19]. The major cause of lung cancer is tobacco smoking, which is the etiology for about 80–85% of lung cancer cases [18], but causes also include previous lung disease [20] and genetics. Genes associated with lung cancer predisposition exhibit a heritability of 18% [21] and the risk of developing lung cancer increases in non-smokers by roughly 1.5-fold when they have a relative with lung cancer [22].

The four main histological types of lung cancer are adenocarcinoma, squamous cell carcinoma, large cell carcinoma, and small cell lung carcinoma, which is the most aggressive type [18]. Treatment of early-stage lung cancer primarily involves surgery [23] following perioperative chemotherapy [24] or both thoracic radiotherapy and chemotherapy, which causes many side effects [25,26]. Antibody-directed therapies have shown promise as a treatment, especially for advanced lung cancer [27–30], but the toxic effects of these approaches remain an issue [29–32]. With a 10–20% survival rates within 5 years [33,34], this cancer type requires effective strategies for detection, prevention, and treatment.

Since the discovery of cisplatin and its anti-proliferative properties, more studies have been conducted on the application of metal complexes in cancer therapy [35]. When a metal coordinates with organic compounds, these coordination complexes can be more effective than precursor organic molecules [36]. For example, the ternary copper (II) valproic acid complex increased the anti-convulsant activity of valproic acid in mice more than three thousand times compared to valproic acid alone [37]. Studies have also shown that coordination complexes can increase the anti-tumoral activity of drugs [38–41]. The high affinity of valproate for transition metals results in stable coordination compounds [42]. In other hand, 2,2-bipyridine (Bipy) is a strong neutral metal binder and a known DNA intercalator. Nicotinamide (Nic) is a great metal binder like Bipy, but is an endogenous non-toxic compound (vitamine B3). Based on these previous studies, this study sought to examine the efficacy of two Zn^{+2} complexes of the antiepileptic drug valproic acid and two different pyridine based neutral binder in inhibiting proliferation of lung cancer cells.

2. Material and methods

2.1. Chemicals

Sodium valproate was purchased from AK Scientific, California, USA. Nicotinamide, 2,2′-bipyridine, absolute ethanol and N,N′-dimethylformamide were purchased from Sigma-Aldrich.

2.2. Physical measurements

^{1}H and ^{13}C NMR analyses were performed using a Fourier 300 spectrometer (Bruker) (300.18 MHz from ^{1}H and 75.49 MHz from ^{13}C with 5 mm probe). Infrared analysis was performed using a Perkin Elmer Spectrum 400 FTIR spectrometer via the KBr pellet method. UV–Vis analysis was performed on a Beckman DU®530 spectrophotometer with a 10 mm quartz cuvette and all solutions were prepared in THF. Melting points were measured using a Quimis® optical apparatus using the glass capillary method. Crystallographic analyses were performed on a Bruker D8 Venture Photon 100 diffractometer.

2.3. Synthesis of zinc (II) complexes

2.3.1. Preparation of precursor tetrakis-μ-2-propylpentanoate dizinc(II) [$Zn_2(Valp)_4$]

Dimeric zinc valproate salt (Scheme 1) was obtained according to Dos Santos (2015) [36]. A solution of $Zn(NO_3)_2$ (2.658 g, 14 mmol) in water (20 mL) was added dropwise over sodium valproate solution (4.650 g, 28 mmol, 100 mL) and maintained with vigorous stirring for 1 h at room temperature. White greasy solid immediately formed and was recovered by filtration and dried over vacuum for 24 h. Yield: 3.41 g (71%); MP: 65° C; ^{1}HNMR (δ-ppm, $DCCl_3$): 0.877 (t-6H, $2CH_3$, $J_{H\text{-}H} = 7$ Hz), 1.720 (m-4H, $2CH_2$, JH-H = 7 Hz), 1.405 and 1.470 (2 m-4H, $2CH_2$, $J_{H\text{-}H} = 8$ Hz), 2.394 (m-1H, CH, $J_{H\text{-}H} = 5$ Hz); ^{13}CNMR (δ-ppm, $DCCl_3$): 14.01 ($2CH_3$), 20.64 ($2CH_2$), 35.07 ($2CH_2$), 47.44 (CH), 186.22 (COO^-); IR (cm^{-1}, KBr pellet): 3423, 2959, 2934, 2873, 1621, 1552, 1528, 1455, 1427, 1379, 1329, 1229, 1121, 1112, 874, 757, 526; 1598 (ν_{as} COO^-), 1427 (ν_s COO^-), (Δv COO^-) 171.UV–Vis (λ-nm, THF): $243_{(weak)}$.

2.3.2. Preparation of bis-(2-propylpentanoate)2,2′-bipyridine zinc(II) [Zn(Valp)$_2$Bipy] (1)

Complex 1 was prepared according to Dos Santos (2015) method [36]. A solution of 2,20 -bipy (11.4 mmol) in DMF (10 mL) was added to a solution of $Zn_2(Valp)_4$ (5.7 mmol) in DMF (10 mL) under vigorous stirring for 20 min. After 24 h, a white solid was formed, which was filtered and dried under vacuum for 12 h. Compound 1 : Yield: 59%; MP: 150C. ^{1}HNMR (δ-ppm, $DCCl_3$): 0.75 (t-12H, $4CH_3$, $J_{H\text{-}H} = 6$ Hz), 1.21 (m-4H, $2CH_2$, $J_{H\text{-}H} = 7$ Hz), 1.51 (m-4H, $2CH_2$, $J_{H\text{-}H} = 8$ Hz), 2.32 (m-2H, 2CH, $J_{H\text{-}H} = 6$ Hz), 7.49 (t-2H, 2CH, $J_{H\text{-}H} = 6$ Hz), 7.98 (t-2H, 2CH, $J_{H\text{-}H} = 9$ Hz), 8.16 (d-2H, 2CH, $J_{H\text{-}H} = 9$ Hz), 8.90 (d-2H, 2CH, $J_{H\text{-}H} = 3$ Hz); ^{13}CNMR (δ-ppm, $DCCl_3$): 14.05 (CH_3), 20.67 (CH_2), 35.38 (CH_2), 46.01 (CH), 120.88 (CH_{ring}), 125.94 (CH_{ring}), 140.12 (CH_{ring}), 148.96 (CH_{ring}), 149.63 (C_{ring}), 186.09 (COO^-); IR (cm^{-1}, KBr pellet): 3109, 3078, 3032, 2955, 2931, 2870, 1607 (ν_{as} COO^-), 1554, 1491, 1444 (ν_s COO^-), 1422, 781, (Δν COO^-) 163; UV–Vis (λ-nm, THF): 295.

2.3.3. Preparation of bis-(2-propylpentanoate)bis-(nicotinamide)zinc(II) [Zn(Valp)$_2$(Nic)$_2$] (2)

Nicotinamide (0.488 g, 4 mmol, 10 mL 99% ethanol) was added dropwise to a vigorously stirred solution of [$Zn_2(Valp)_4$] (0.703 g, 1 mmol) in absolute ethanol (10 mL). The clear solution was stirred for 60 min and concentrated to 20% of the start volume by vacuum at 50 °C. Clear scale-like crystals were obtained after 3 days, filtered and washed in 99% ethanol, and freeze dried for 24 h. Compound 2: Yield: 0.834 g (70%); MP: 155° C; ^{1}HNMR (δ-ppm, Acetone D_6): 0.865 (t-12H, $4CH_3$, $J_{H\text{-}H} = 7$ Hz), 1.309 (m-8H, $4CH_2$, $J_{H\text{-}H} = 9$ Hz), 1.361 and 1.526 (2 m-8H, $4CH_2$, $J_{H\text{-}H} = 5$ Hz), 2.330 (m-2H, 2CH, $J_{H\text{-}H} = 5$ Hz), 6.921 (s-2H, $2NH_{(Nic)}$), 7.506 (m-2H, $2CH_{(Nic)}$, $J_{H\text{-}H} = 5$ Hz), 7.735 (s-2H, $2NH_{(Nic)}$), 8.274 (m-2H, $2CH_{(Nic)}$, $J_{H\text{-}H} = 8$ Hz), 8.720 (m-2H, $2CH_{(Nic)}$, $J_{H\text{-}H} = 5$ Hz), 9.129 (m-2H, $2CH_{(Nic)}$, $J_{H\text{-}H} = 2$ Hz); ^{13}CNMR (δ-ppm, Acetone D_6): 14.433 ($4CH_3$), 21.411 ($4CH_2$), 36.015 ($4CH_2$), 124.226 ($2CH_{(Nic)}$), 130.853 ($2CH_{(Nic)}$), 136.229 ($2CH_{(Nic)}$), 149.748 ($2CH_{(Nic)}$), 152.822 ($2C_{(Nic)}$), 167.379 ($2CON_{(Nic)}$); IR (cm^{-1}, KBr pellet): 3325, 3166, 3075, 2957, 2934, 2872, 2859, 2789, 1695, 1640, 1605, 1465, 1456, 1436, 1385, 1322, 1294, 1228, 1201, 1155, 1118, 1051, 1034, 951, 870, 844, 807, 793, 757, 702, 655, 513. 1559 (ν_{as} COO^-), 1425 (ν_s COO^-), (Δν COO^-) 134; UV–Vis (λ-nm, THF): 259.5.

2.4. Crystallography

Single-crystal X-ray diffraction data for complex 2 were collected on a Bruker D8 Venture Photon 100 diffractometer equipped with an Incoatec IμS high brilliance Mo-Kα X-ray tube with two-dimensional Montel micro-focusing optics (120(2) K using an Oxford Cryosystems Cryostream 800 low temperature unit for complex 2). The structure was directly solved using SHELXS [43]. Subsequent difference Fourier map analyses yielded the positions of the non-hydrogen atoms. All

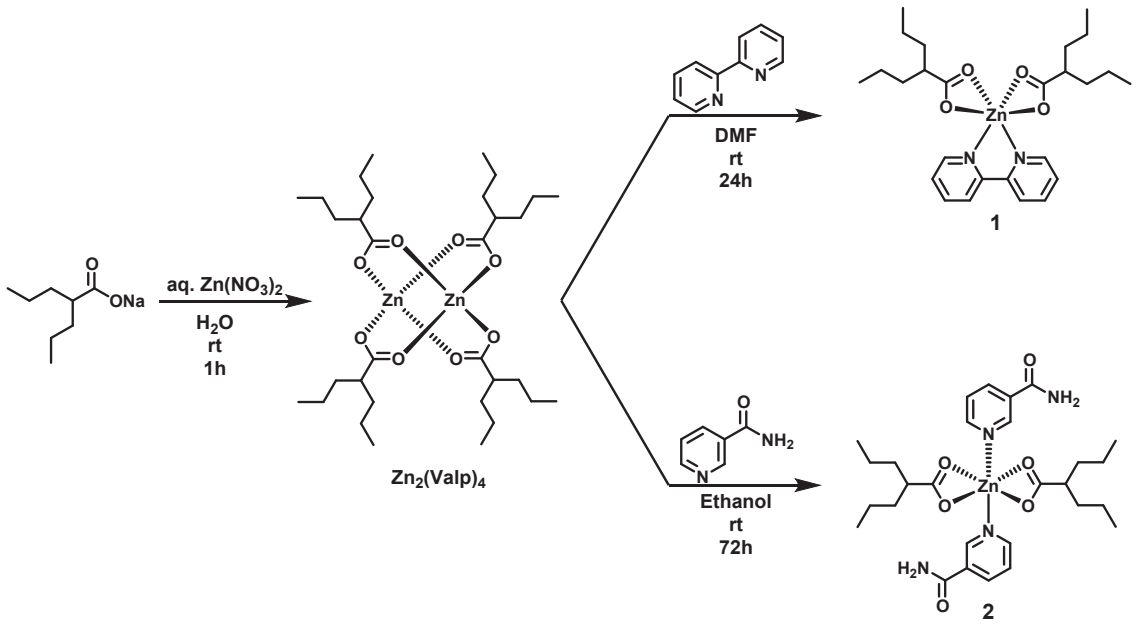

Scheme 1. Two step synthesis of complexes **1** and **2**.

refinements were made by full-matrix least-squares on F2 with anisotropic displacement parameters for all non–hydrogen atoms using the SHELXL package. Hydrogen atoms were accounted for during analysis while the calculated positions were being refined, but the hydrogen atoms that had special bonds were located in the Fourier map. Drawings were created using ORTEP-3.1 for Windows and Mercury 4.1.0.44.

2.5. Cell lines

The cell lines A549 (adenocarcinoma human alveolar basal epithelial cells) and Vero CCL81 (*Cercopithecus aethiops* kidney normal) were purchased from the American Type Culture Collection (ATCC). A549 cells were cultured in DMEM F12 medium supplemented with 10% fetal bovine serum (FBS). Vero cells were cultured in DMEM high glucose with 10% FBS. All cells were incubated at 5% CO_2 and 37 °C. All experiments were performed using freshly thawed cells after three passages. Cell lines were tested for Mycoplasma contamination.

2.6. Cytotoxicity assay

Cells were seeded in 96-well flat-bottom plates at concentrations of $5x10^3$ cells/well for A549 cells and $2x10^3$ cells/well for Vero cells, according Denizot & Lang (1986) [44]. After 24 h of incubation, 250.0, 137.5, 25.0, 13.75 or 2.5 μmol L^{-1} of **1** or **2** was added and the plates were incubated for an additional 24 h at 37 °C in a humidified incubator with 5% CO_2. For the vehicle control, DMSO was added in the same volumes that were used to dilute the complexes. As an additional negative control (NC), untreated cells were also assayed. Cell viability was assessed using a colorimetric assay based on the reduction of 3-[4,5-dimethylthiazol-2-y1]-2,-diphenyltetrazolium bromide (MTT) by mitochondrial enzymes (Molecular Probes™, Thermo Fisher Scientific, Waltham, MA, USA). Briefly, 100 μL of medium was removed and 40 μL of MTT reagent (5 mg mL^{-1}) was added into each well. Cells were incubated for 2.5 h and the precipitated formazan crystals were dissolved in dimethyl sulfoxide (DMSO). Finally, the optic density (OD) was analyzed at 570/620 nm using a micro-plate reader (EZ Read 400, Biochrom). Assays were performed in triplicate. For cytotoxicity calculation, the OD of the treated cells was multiplied by the percentage equivalent to the cells treated with DMSO, and then divided by the OD of the cells treated with DMSO.

2.7. Clonogenic assay

A549 cells were treated for 24 h with each compound, then plated in a new 6-well plate at a concentration of 500 cells/well. After 11 days, with a change in medium at day 5, the wells were washed with phosphate buffered saline (PBS) and fixed with 4% paraformaldehyde for 10 min. Cells were then washed with PBS and incubated overnight at 37 °C and 5% CO_2 to dry the wells. Cells were then stained with 60% Giemsa 10% ethanol solution. Colonies were counted and graphs were plotted in GraphPad Prism Version 5.00 (GraphPad Software Inc., CA).

2.8. Cell cycle analysis

A549 cells were treated with 250 μmol L^{-1} of complexes **1** and **2** and NaValp for 24 h. The cells were trypsinized and resuspended in PBS. Then, cells were centrifuged and washed in PBS. Following fixation in cold 70% ethanol for 20 min at −20 °C, the cells were washed with PBS and staining buffer and then stained with 7-amino- actinomycin (7-AAD, 5 μL) for 15 min at room temperature. The stained cells were subjected to cell cycle analysis using FACS Canto II (BD Biosciences).

2.9. Apoptosis analysis

Annexin V/PI analyses were carried out using the FITC Annexin V/PI apoptosis/necrosis detection kit (QuatroG). After treatment with 250 μmol L^{-1} of complexes **1** and **2** and NaValp for 24 h, A549 cells were washed in cold PBS, resuspended in 1X binding buffer, and incubated with FITC annexin V (200 μg mL^{-1}) and propidium iodide (40 μg mL^{-1}) for 15 min at room temperature. Following incubation, cells were washed with PBS and analyzed by FACS Canto II (BD Biosciences).

2.10. Data analysis

The half maximal inhibitory concentrations (IC50) of compounds and controls were calculated using linear and polynomial regression analyses. The IC50 values were reported as a mean of three independent experiments. The selectivity index (SI) was calculated according to the following equation: SI = IC50 of Vero cells/ IC50 of tumor cells. Statistical analyses were performed with GraphPad Prism (GraphPad Software Inc., CA) using two-way ANOVA followed by Bonferroni

correction.

3. Results and discussion

3.1. Crystallographic study of complex 2

Crystallization of complex 2 occurs in a monoclinic system with space group (type *C*2/*c*) (Table 1), a common molecular packaging unit for Zn complexes containing valproate and pyridine derivatives as described by ABU, et al. (2013) [45]. Fig. 1 shows the structure (ORTEP) of complex 2 based on the assumption that the central Zn II atom is linked to four oxygen atoms from two valproate groups and two nitrogen atoms from two nicotinamide groups. The coordination sphere is formed by a distorted octahedron with two nicotinamide molecules arranged at an angle of 96.08° (Table 2) from each other opposite to two bidentate valproate molecules. The oxygen atoms of the carboxylate group bind asymmetrically to the metal through a 2.090 Å bond with a valence oxygen and 2.3108 Å bond with the carbonyl oxygen.

The representation of the intermolecular structure of complex 2 in Fig. 2 shows cohesive molecular packaging through hydrogen bonds. Each nicotinamide binder produces three intermolecular H-bonds, two of which are symmetrical to each other in reference to the amide groups (2.048 Å) (NHO) and the third occurring between the hydrogen of the amide group and the carbonyl oxygen of a valproate group of the neighboring molecule 2,118 Å away.

3.2. Antitumor analysis complexes 1 and 2

Cytotoxic effects of complexes **1** and **2** were tested against human lung adenocarcinoma cells (A549). Cells were exposed to different concentrations of complexes 1 or 2 (i.e., 250.0, 137.5, 25.0, 13.75, or 2.5 μmol L^{-1}). Controls were treated with valproate in the same concentrations (Fig. 3A).

Table 1
Crystallographic parameters for complex 2.

Parameters	Results
Empirical formula	$C_{28}H_{42}N_4O_6Zn$
Formula weight	596.03
T / K	293(2)
Radiation, l / Å	Mo Kα; 0.71073
Crystal system, space group	Monoclinic, *C*2/*c*
Unit cell (Å) dimensions*A*	
A	14.4173(5)
B	10.4246(4)
C	20.7978(8)
α(°)	90
β (°)	98.2030(10)
γ (°)	90
V (Å)	3093.8(2)
Z, Calculated density (g.cm^{-3})	4, 1.280
Absorption coefficient (mm^{-1})	0.838
F (000)	1264
Crystal size (mm)	0.20 × 0.12 × 0.11
Theta range for data collection	3.25 to 30.60 deg.
Index ranges	$-17\leq h\leq 20$ $-14\leq k\leq 14$ $-29\leq l\leq 22$
Reflections collected / unique	11,878 / 4757 [R(int) = 0.0151]
Completeness to the theta max (30.60)	99.8 %
Absorption correction	Semi-empirical from equiequivalents equivalents
Max. and min. transmission	0.9235 and 0.8703
Refinement method	Full-matrix least-squares on F^2
Data / restraints / parameters	4757/20/171
Goodness-of-fit on F^2	1.032
Final *R* indices [$I > 2\sigma(I)$]	R1 = 0.0564, w*R*2 = 0.1539
R indices	R1 = 0.0710, w*R*2 = 0.1627
Largest diff. peak and hole (e.$Å^{-3}$)	1.146 and −1.137

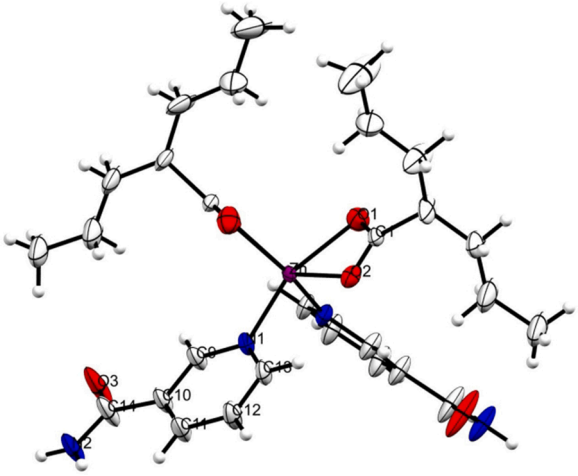

Fig. 1. ORTEP of complex **2** representing an octahedral coordination sphere.

Table 2
Main bond lengths and angles of complex 2.

Bond	Length (Å)	System	Angle (°)
Zn-N(1)	2.086(2)	N(1)-Zn-N(1)#1	96.08(12)
Zn-N(1)#1	2.086(2)	N(1)-Zn-O(1)	149.55(9)
Zn-O(1)	2.090(2)	N(1)#1-Zn-O(1)	90.67(9)
Zn-O(1)#1	2.090(2)	N(1)-Zn-O(1)#1	90.67(9)
Zn-O(2)	2.311(18)	N(1)#1-Zn-O(1)#1	149.55(9)
Zn-(O)2#1	2.311(19)	O(1)-Zn-O(1)#1	98.39(12)
Zn-C(1)	2.543(2)	N(1)-Zn-O(2)	90.91(8)
Zn-C(1)#1	2.543(2)	N(1)#1-Zn-O(2)	110.26(7)
		O(1)-Zn-O(2)	59.03(8)
		O(1)#1-Zn-O(2)	99.24(8)
		N(1)-Zn-O(2)#1	110.26(7)
		O(3)-C(14)-N(2)	123.1(3)

Complex **1** exhibited greater cytotoxic effects than complex **2** and the valproate control in A549 cells (Fig. 3A). When administered in concentrations ranging from 25 μM to 250 μM, complex **1** significantly reduced cellular viability compared to valproate (Fig. 3A). Complex **2** also significantly reduced A549 cellular viability, but only when added in the highest concentration of 250 μM (Fig. 3A).

We also evaluated the selectivity of the cytotoxic effects of complexes **1** and **2** using a non-tumor cell line (Vero). We found that complex **2** exhibited less cytotoxicity in Vero cells compared to complex **1** when it was applied in concentrations of 137.5 μM and 250 μM (Fig. 3B). Table 3 shows the IC50 of each complex. Complex **1** exhibited the lowest IC50 compared to valproate and complex **2,** indicating that complex **1** had the greatest cytotoxic effects. However, complex **1** also had a low IC50 value in Vero cells, which indicate that although complex **1** is effective in inhibiting tumor cell growth, it is not selective. This data is confirmed by the selectivity indices (SI) present in Table 4, which show an SI < 1 for complex **1**. Complex **2** presented higher values of SI, indicating that it was more selective than **1** (Table 4).

Using a clonogenic assay, we further investigated the capacity of A549 cells to proliferate after treatment with NaValp, complexes **1** or **2**. We used concentrations of 250 μmol L^{-1} for both complexes and NaValp. Both complexes **1** and **2** did not significantly affect cell proliferation compared to NaValp (Fig. 4).

To investigate the effects of NaValp, complex **1** or **2** on tumor cell death, apoptosis was analyzed via annexin V assays. We found that complex **1** caused more apoptosis than complex **2** and NaValp (Fig. 5A, B and C). To observe if any of the compounds affected cell cycle dynamics, flow cytometry using 7-AAD dye was performed. A549 cells were treated for 24 h and then harvested and labeled. Complex **2** and valproate caused a reduction in cells in S phase compared to the DMSO, negative

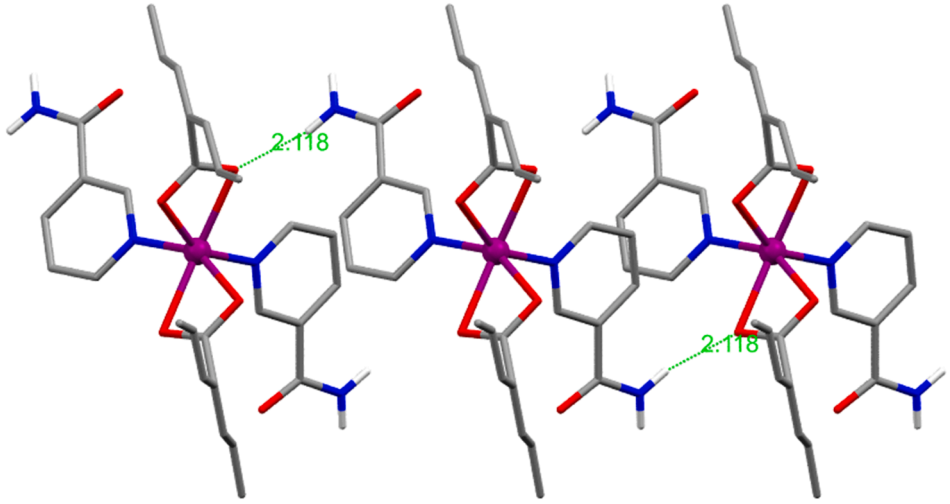

Fig. 2. Intermolecular H-bond spatial system of complex **2**.

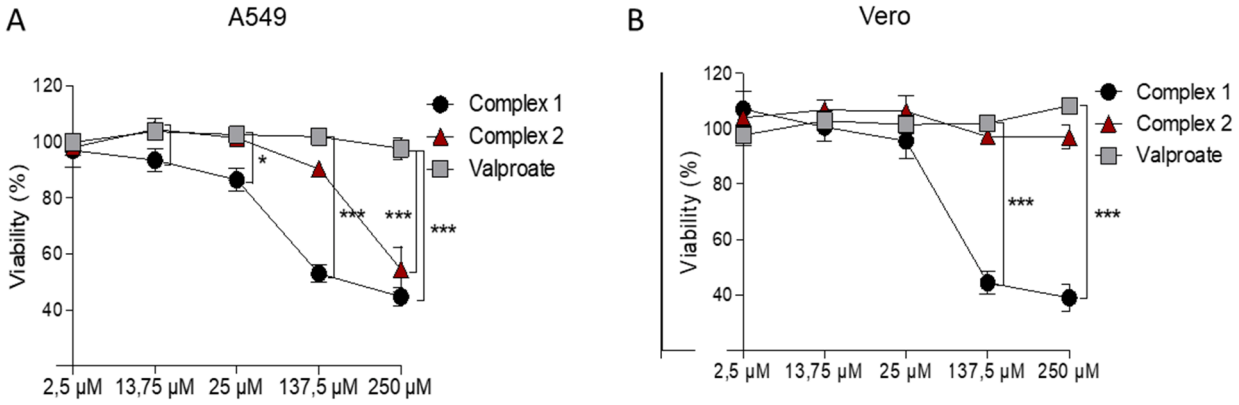

Fig. 3. Cytotoxicity of complex 1, complex 2, and valproate in (a) A549 cells and (b) Vero cells. Cell viability was assessed via MTT assay. Dose response curves represent viability 24 h after treatment with 2.5–250 µmol L^{-1} of each compound. Values represent the mean and standard deviation of three independent replicates. * indicates p-values lower than 0.05 and *** indicates p-values lower than 0.001.

Table 3
Cytotoxic activities (IC50) of NaValp, complexes 1 and 2.

Cell line	IC50 (µmol L^{-1})		
	1	2	NaValp
A549	205.66	310.66	3053.51
Vero	190.70	1537.30	1759.20

Table 4
Selectivity indices (SI) of NaValp, complexes 1 and 2.

Cell line	SI (µmol L^{-1})		
	1	2	NaValp
A549	0.92	5.60	0,63

control and cells treated with complex **1** (Fig. 6A and B).

Cancer is one of the leading causes of death in the developed world. Lung cancer especially cause high mortality rates and is prevalent worldwide [46]. Consequently, several studies have been conducted to characterize the anti-proliferative effects of various classes of compounds, ranging from naturally occurring molecules and their derivates to inorganic or coordination compounds. In this study, we described the cytotoxic effects of two zinc(II) complexes with sodium valproate,

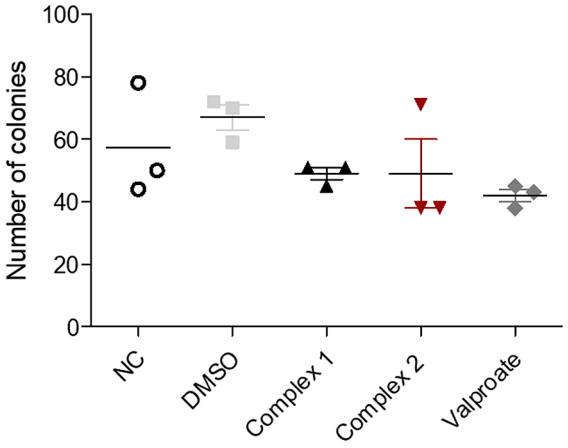

Fig. 4. Clonogenic assay of A549 cells treated with complexes 1 and 2 and NaValp. Cells were treated, incubated for 24 h, washed twice, and plated for clonogenic assays. Colonies were counted 11 days afterward.

complexes **1** and **2**, and found that they are more cytotoxic than NaValp alone in lung adenocarcinoma cell lines. Valproate is a histone deacetylase inhibitor and exhibits antitumor properties, which have been

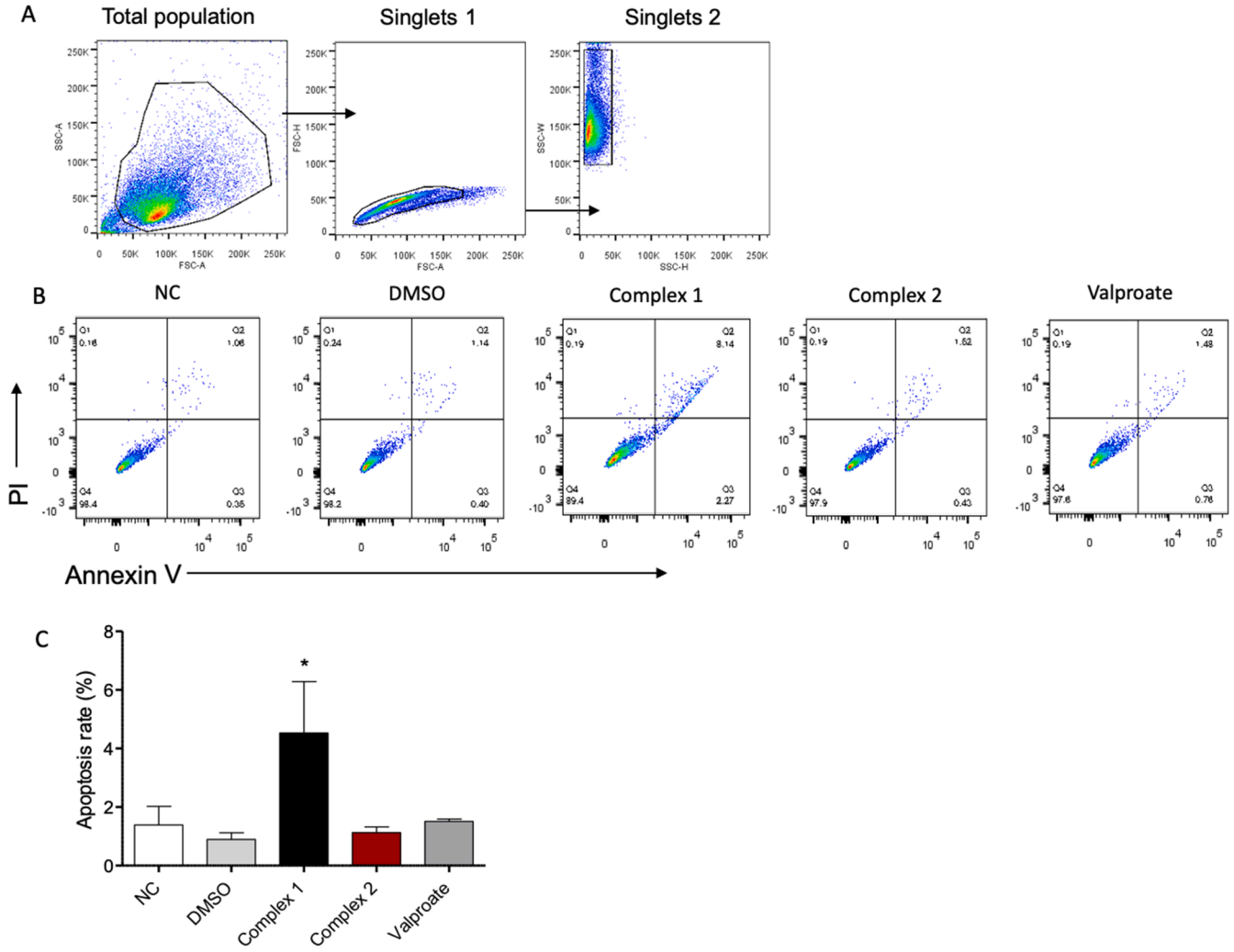

Fig. 5. The effects of complex 1, complex 2, and valproate on apoptosis. A549 cells were double stained with annexin V and PI and analyzed using flow cytometry. (A) Gate of cells. (B) Four populations were identified: non-apoptotic dead cells (Q1), late apoptotic cells (Q2), viable cells (Q4), and early apoptotic cells (Q3). (C) % of annexin V + PI + A549 cells 24 h after compound application. * indicates p-values lower than 0.05.

demonstrated in different tumor models and clinical trials [47,48]. In a phase II trial, valproate, when used in association with other drugs, provided clinical benefits for 12 of 15 patients (80%) with different tumor types, including lung cancer [49]. Adjunctive therapeutic use of valproate has already been tested in patients with cisplatin-resistant ovarian cancer and cervical cancer with recurrent metastasis in phase III trials, among other types of cancer in phase I/II trials [50]. A combination of magnesium valproate and hydralazine was also approved for use in cervical cancer in Mexico [51].

We demonstrated that complexes **1** and **2** cause a significant reduction in growth of human lung cells (A549) compared to NaValp, suggesting that the addition of Zn complexes improves the cytotoxic effects of valproate. However, complex **2** was more selective to tumor cells compared to complex **1**.

The cytotoxic effects of NaValp (1 mmol L^{-1}) were previously evaluated in the lung cancer cell line A549, which resulted in a reduction in 20% of cell growth after 5 days of treatment [15]. In the present work, valproate did not reduce the viability of A549. However, we used a lower concentration of NaValp (250 μmol L^{-1}), which may explain the discordance in findings. In contrast, Hao 2017 observed a significant 20% increase in A549 cell death by apoptosis after applying 1 μmol L^{-1} concentrations of valproate [52]. The differences between our data may be associated with the sensitivity of our detection methods since we found that 250 μmol L^{-1} concentrations of valproate promote around 2% cell death. However, in agreement with our findings, Hao 2017 detected lower rates of A549 cells in S phase after valproate treatment. Gavrilov 2015 also described the reduction of cells in the pre-G1 phase of the cell cycle after treatment with 1000 μmol L^{-1} valproate [15].

4. Conclusion

Although complex 2 reduced the viability of A549 cells and the cell cycle S phase, it did not induce apoptosis. As such, the mechanisms by which complexes **1** and **2** decrease the cell viability of this cell lineage are likely different. Complex **1** primarily caused cell death by inducing apoptosis. In contrast, complex **2** only regulated cell cycle, which may not be the only mechanism by which complex **2** caused reduced viability. This phenomenon can be attributed to the known cytotoxic effect of the bipy group present in complex **1**, a DNA intercalating agent while complex **2** has Nic groups as *n*-donor moiety, a known biological compound with function and more tolerable to the cellular machinery.

In summary, our results demonstrated that complexes **1** and **2** are more effective than NaValp in reducing cellular growth of A459, highlighting the potential antitumoral activity of compounds derived from valproate-Zn^{+2} complexes.

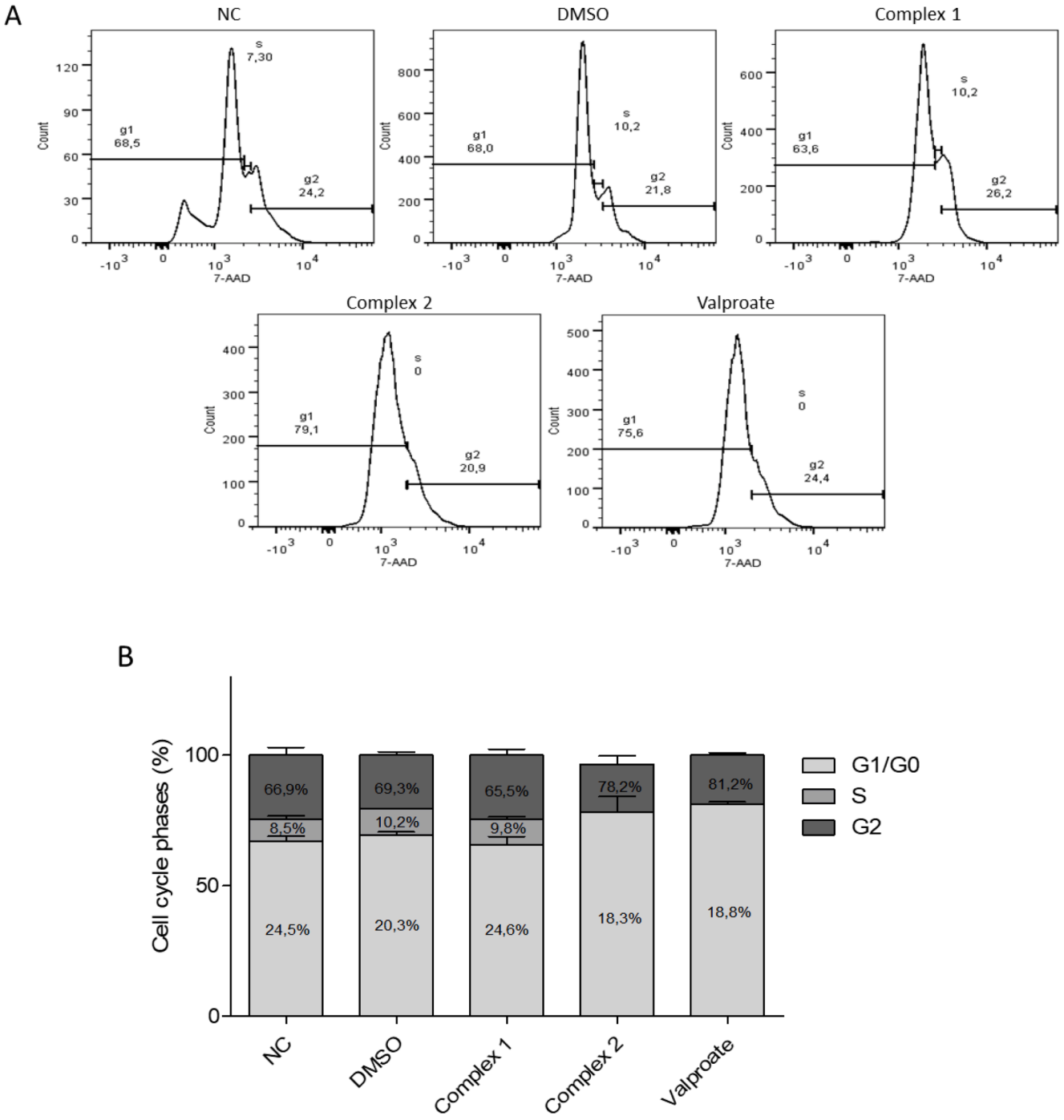

Fig. 6. The effect of complexes 1 and 2 and valproate on cell cycle. A549 cells were treated and incubated for 24 h and dyed with 7-AAD. Cells were analyzed on a BD FACS Canto III. (A) Histograms of 7-AAD stained cells showing cell cycle phases. (B) Quantification of cell populations in G0/G1, G2/M and S phases.

CRediT authorship contribution statement

Emanuelle Fraga da Silva: Formal analysis, Investigation, Writing - original draft. **Paulo Roberto dos Santos:** Investigation, Formal analysis, Writing - original draft. **Krist Helen Antunes:** Investigation, Formal analysis. **Caroline Marinho Franceschina:** Investigation. **Deise Nascimento de Freitas:** Investigation. **Priscila Konrad:** Investigation. **Rafael Fernandes Zanin:** Conceptualization, Project administration. **Pablo Machado:** Conceptualization, Project administration. **Sidnei Moura:** Conceptualization, Writing - original draft, Supervision, Project administration, Funding acquisition. **Ana Paula Duarte de Souza:** Conceptualization, Writing - original draft, Supervision, Project administration, Funding acquisition.

Declaration of Competing Interest

The authors declare that they have no known competing financial interests or personal relationships that could have appeared to influence the work reported in this paper.

Acknowledgements

Thanks to UCS-Caxias do Sul, PUC Porto Alegre and La Salle University-Canoas. Especial thanks to CAPES for scholarships (Financial

code 1). Thanks to Professor Davi Bach (Federal University of Santa Maria) for crystallographic studies. FAPERGS 16/2551-0000523-0.

Appendix A:. Supplementary data

CCDC-1912928 contain the supplementary crystallographic data for the complexes **2**. These data can be obtained free of charge via http://www.ccdc.cam.ac.uk/conts/retrieving.html, or from the Cambridge Crystallographic Data Center, 12 Union Road, Cambridge CB2 1EZ, UK; fax: (+44) 1223–336–033; or e–mail: deposit@ccdc.cam.ac.uk.

Appendix B. Supplementary data

Supplementary data to this article can be found online at https://doi.org/10.1016/j.poly.2021.115415.

References

[1] M. Romoli, P. Mazzocchetti, R. D'Alonzo, S. Siliquini, V.E. Rinaldi, A. Verrotti, P. Calabresi, C. Costa, Valproic acid and epilepsy: from molecular mechanisms to clinical evidences, Curr. Neuropharmacol. 17 (10) (2019) 926–946, https://doi.org/10.2174/1570159X17666181227165722.

[2] J. Hayes, P. Prah, I. Nazareth, M. King, K. Walters, I. Petersen, D. Osborn, J. Laks, Prescribing trends in bipolar disorder: Cohort study in the united kingdom thin primary care database 1995–2009, PLoS One 6 (12) (2011) e28725, https://doi.org/10.1371/journal.pone.002872510.1371/journal.pone.0028725.g00110.1371/journal.pone.0028725.g00210.1371/journal.pone.0028725.g00310.1371/journal.pone.0028725.g00410.1371/journal.pone.0028725.g00510.1371/journal.pone.0028725.g00610.1371/journal.pone.0028725.t00110.1371/journal.pone.0028725.t002.

[3] K. Lipska, A. Gumieniczek, A.A. Filip, Anticonvulsant valproic acid and other short-chain fatty acids as novel anticancer therapeutics: Possibilities and challenges, Acta Pharm. 70 (2020) 291–301, https://doi.org/10.2478/acph-2020-0021.

[4] C. Zhuo, Z. Xun, W. Hou, F. Ji, X. Lin, H. Tian, W. Zheng, M. Chen, C. Liu, W. Wang, C. Chen, Surprising anticancer activities of psychiatric medications: Old drugs offer new hope for patients with brain cancer, Front. Pharmacol. 10 (2019) 1–7, https://doi.org/10.3389/fphar.2019.01262.

[5] N. Batty, G.G. Malouf, J.P.J. Issa, Histone deacetylase inhibitors as anti-neoplastic agents, Cancer Lett. 280 (2) (2009) 192–200, https://doi.org/10.1016/j.canlet.2009.03.013.

[6] C.L. Bacon, H.C. Gallagher, J.C. Haughey, C.M. Regan, Antiproliferative action of valproate is associated with aberrant expression and nuclear translocation of cyclin D3 during the C6 glioma G1 phase, J. Neurochem. 83 (2002) 12–19, https://doi.org/10.1046/j.1471-4159.2002.01081.x.

[7] W. Weichert, HDAC expression and clinical prognosis in human malignancies, Cancer Lett. 280 (2) (2009) 168–176, https://doi.org/10.1016/j.canlet.2008.10.047.

[8] J.J. Cinatl, J. Cinatl, P.H. Driever, R. Kotchetkov, P. Pouckova, B. Kornhuber, D. Schwabe, Sodium valproate inhibits in vitro growth of human neuroblastoma cells, Anticancer. Drugs 8 (1997) 958–963, https://doi.org/10.1097/00001813-199711000-00007.

[9] A. Avallone, M.C. Piccirillo, P. Delrio, B. Pecori, E. Di Gennaro, L. Aloj, F. Tatangelo, V. D'Angelo, C. Granata, E. Cavalcanti, N. Maurea, P. Maiolino, F. Bianco, M. Montano, L. Silvestro, M. Terranova Barberio, M.S. Roca, M. Di Maio, P. Marone, G. Botti, A. Petrillo, G. Daniele, S. Lastoria, V.R. Iaffaioli, G. Romano, C. Caracò, P. Muto, C. Gallo, F. Perrone, A. Budillon, Phase 1/2 study of valproic acid and short-course radiotherapy plus capecitabine as preoperative treatment in low-moderate risk rectal cancer-V-shoRT-R3 (Valproic acid - short RadioTherapy - rectum 3rd trial), BMC Cancer 14 (2014) 1–12, https://doi.org/10.1186/1471-2407-14-875.

[10] M.G. Catalano, M. Pugliese, M. Gallo, E. Brignardello, P. Milla, F. Orlandi, P. P. Limone, E. Arvat, G. Boccuzzi, A. Piovesan, Valproic Acid, a Histone Deacetylase Inhibitor, in Combination with Paclitaxel for Anaplastic Thyroid Cancer: Results of a Multicenter Randomized Controlled Phase II/III Trial, Int. J. Endocrinol. 2016 (2016) 1–8, https://doi.org/10.1155/2016/2930414.

[11] A. Chavez-Blanco, B. Segura-Pacheco, E. Perez-Cardenas, L. Taja-Chayeb, L. Cetina, M. Candelaria, D. Cantu, A. Gonzalez-Fierro, P. Garcia-Lopez, P. Zambrano, C. Perez-Plasencia, G. Cabrera, C. Trejo-Becerril, E. Angeles, A. Duenas-Gonzalez, Histone acetylation and histone deacetylase activity of magnesium valproate in tumor and peripheral blood of patients with cervical cancer. A phase I study, Mol. Cancer 4 (2005) 1–9, https://doi.org/10.1186/1476-4598-4-22.

[12] A.I. Daud, J. Dawson, R.C. Deconti, E. Bicaku, D. Marchion, S. Bastien, F. A. Hausheer, R. Lush, A. Neuger, D.M. Sullivan, P.N. Munster, Potentiation of a topoisomerase i inhibitor, karenitecin, by the histone deacetylase inhibitor valproic acid in melanoma: translational and phase l/ll clinical trial, Clin. Cancer Res. 15 (2009) 2479–2487, https://doi.org/10.1158/1078-0432.CCR-08-1931.

[13] J.-P. Issa, G. Garcia-Manero, X. Huang, J. Cortes, F. Ravandi, E. Jabbour, G. Borthakur, M. Brandt, S. Pierce, H.M. Kantarjian, Results of phase 2 randomized study of low-dose decitabine with or without valproic acid in patients with myelodysplastic syndrome and acute myelogenous leukemia, Cancer 121 (4) (2015) 556–561, https://doi.org/10.1002/cncr.29085.

[14] O. Akgun, M. Erkisa, F. Ari, Effective and new potent drug combination: Histone deacetylase and Wnt/β-catenin pathway inhibitors in lung carcinoma cells, J. Cell. Biochem. 120 (9) (2019) 15467–15482, https://doi.org/10.1002/jcb.v120.910.1002/jcb.28813.

[15] V. Gavrilov, K. Lavrenkov, S. Ariad, S. Shany, Sodium valproate, a histone deacetylase inhibitor, enhances the efficacy of vinorelbine-cisplatin-based chemoradiation in non-small cell lung cancer cells, Anticancer Res. 34 (2014) 6565–6572.

[16] B.F. Chu, M.J. Karpenko, Z. Liu, J. Aimiuwu, M.A. Villalona-Calero, K.K. Chan, M. R. Grever, G.A. Otterson, Phase i study of 5-aza-2′-deoxycytidine in combination with valproic acid in non-small-cell lung cancer, Cancer Chemother. Pharmacol. 71 (1) (2013) 115–121, https://doi.org/10.1007/s00280-012-1986-8.

[17] H. Heers, J. Stanislaw, J. Harrelson, M.W. Lee, Valproic acid as an adjunctive therapeutic agent for the treatment of breast cancer, Eur. J. Pharmacol. 835 (2018) 61–74, https://doi.org/10.1016/j.ejphar.2018.07.057.

[18] C.P. Wild, E. Weiderpass, B.W.S. Stewart, World Cancer Report (2020), https://doi.org/10.1016/j.cma.2010.02.010.

[19] F. Bray, J. Ferlay, I. Soerjomataram, R.L. Siegel, L.A. Torre, A. Jemal, Global cancer statistics 2018: GLOBOCAN estimates of incidence and mortality worldwide for 36 cancers in 185 countries, CA. Cancer J. Clin. 68 (2018) 394–424. https://doi.org/10.3322/caac.21492.

[20] Darren R. Brenner, John R. McLaughlin, Rayjean J. Hung, Landon Myer, Previous lung diseases and lung cancer risk: A systematic review and meta-analysis, PLoS One 6 (3) (2011) e17479, https://doi.org/10.1371/journal.pone.001747910.1371/journal.pone.0017479.g00110.1371/journal.pone.0017479.g00210.1371/journal.pone.0017479.g00310.1371/journal.pone.0017479.t00110.1371/journal.pone.0017479.s00110.1371/journal.pone.0017479.s00210.1371/journal.pone.0017479.s00310.1371/journal.pone.0017479.s00410.1371/journal.pone.0017479.s00510.1371/journal.pone.0017479.s00610.1371/journal.pone.0017479.s00710.1371/journal.pone.0017479.s00810.1371/journal.pone.0017479.s00910.1371/journal.pone.0017479.s01010.1371/journal.pone.0017479.s01110.1371/journal.pone.0017479.s01210.1371/journal.pone.0017479.s013.

[21] Jennifer R. Harris, Jacob Hjelmborg, Hans-Olov Adami, Kamila Czene, Lorelei Mucci, Jaakko Kaprio, The Nordic Twin Study on Cancer - NorTwinCan, Twin Res. Hum. Genet. 22 (6) (2019) 817–823, https://doi.org/10.1017/thg.2019.71.

[22] Michele L. Coté, Mei Liu, Stefano Bonassi, Monica Neri, Ann G. Schwartz, David C. Christiani, Margaret R. Spitz, Joshua E. Muscat, Gad Rennert, Katja K. Aben, Angeline S. Andrew, Vladimir Bencko, Heike Bickeböller, Paolo Boffetta, Paul Brennan, Hermann Brenner, Eric J. Duell, Eleonora Fabianova, John K. Field, Lenka Foretova, Søren Friis, Curtis C. Harris, Ivana Holcatova, Yun-Chul Hong, Dolores Isla, Vladimir Janout, Lambertus A. Kiemeney, Chikako Kiyohara, Qing Lan, Philip Lazarus, Jolanta Lissowska, Loic Le Marchand, Dana Mates, Keitaro Matsuo, Jose I. Mayordomo, John R. McLaughlin, Hal Morgenstern, Heiko Müeller, Irene Orlow, Bernard J. Park, Mila Pinchev, Olaide Y. Raji, Hedy S. Rennert, Peter Rudnai, Adeline Seow, Isabelle Stucker, Neonila Szeszenia-Dabrowska, M. Dawn Teare, Anne Tjønnelan, Donatella Ugolini, Henricus F.M. van der Heijden, Erich Wichmann, John K. Wiencke, Penella J. Woll, Ping Yang, David Zaridze, Zuo-Feng Zhang, Carol J. Etzel, Rayjean J. Hung, Increased risk of lung cancer in individuals with a family history of the disease: A pooled analysis from the International Lung Cancer Consortium, Eur. J. Cancer 48 (13) (2012) 1957–1968, https://doi.org/10.1016/j.ejca.2012.01.038.

[23] J. Vansteenkiste, L. Crino, C. Dooms, J.Y. Douillard, E. Lim, G. Rocco, S. Senan, P. Van Schil, G. Veronesi, R. Stahel, S. Peters, E. Felip, P. Members, U. Kingdom, R.B. Hospital, P. Foundation, T. Surgery, Annals of Oncology Advance Access published February 22, 2014, in: 2nd ESMO Consens. Conf. Lung Cancer Early Stage Non-small Cell Lung Cancer Consens. Diagnosis, Treat. Follow., 2014: pp. 1–37.

[24] Jean-Pierre Pignon, Hélène Tribodet, Giorgio V. Scagliotti, Jean-Yves Douillard, Frances A. Shepherd, Richard J. Stephens, Ariane Dunant, Valter Torri, Rafael Rosell, Lesley Seymour, Stephen G. Spiro, Estelle Rolland, Roldano Fossati, Delphine Aubert, Keyue Ding, David Waller, Thierry Le Chevalier, Lung adjuvant cisplatin evaluation: A pooled analysis by the LACE collaborative group, J. Clin. Oncol. 26 (21) (2008) 3552–3559, https://doi.org/10.1200/JCO.2007.13.9030.

[25] W.J. Curran, R. Paulus, C.J. Langer, R. Komaki, J.S. Lee, S. Hauser, B. Movsas, T. Wasserman, S.A. Rosenthal, E. Gore, M. Machtay, W. Sause, J.D. Cox, Sequential vs concurrent chemoradiation for stage iii non-small cell lung cancer: Randomized phase III trial RTOG 9410, J. Natl. Cancer Inst. 103 (19) (2011) 1452–1460, https://doi.org/10.1093/jnci/djr325.

[26] Anne Aupérin, Cecile Le Péchoux, Estelle Rolland, Walter J. Curran, Kiyoyuki Furuse, Pierre Fournel, Jose Belderbos, Gerald Clamon, Hakki Cuneyt Ulutin, Rebecca Paulus, Takeharu Yamanaka, Marie-Cecile Bozonnat, Apollonia Uitterhoeve, Xiaofei Wang, Lesley Stewart, Rodrigo Arriagada, Sarah Burdett, Jean-Pierre Pignon, Meta-analysis of concomitant versus sequential radiochemotherapy in locally advanced non - small-cell lung cancer, J. Clin. Oncol. 28 (13) (2010) 2181–2190, https://doi.org/10.1200/JCO.2009.26.2543.

[27] Michael A. Postow, Margaret K. Callahan, Jedd D. Wolchok, Immune checkpoint blockade in cancer therapy, J. Clin. Oncol. 33 (17) (2015) 1974–1982, https://doi.org/10.1200/JCO.2014.59.4358.

[28] Achim Rittmeyer, Fabrice Barlesi, Daniel Waterkamp, Keunchil Park, Fortunato Ciardiello, Joachim von Pawel, Shirish M Gadgeel, Toyoaki Hida, Dariusz M Kowalski, Manuel Cobo Dols, Diego L Cortinovis, Joseph Leach, Jonathan Polikoff, Carlos Barrios, Fairooz Kabbinavar, Osvaldo Arén Frontera, Filippo De Marinis, Hande Turna, Jong-Seok Lee, Marcus Ballinger, Marcin Kowanetz, Pei He, Daniel S Chen, Alan Sandler, David R Gandara, Atezolizumab versus docetaxel in patients with previously treated non-small-cell

lung cancer (OAK): a phase 3, open-label, multicentre randomised controlled trial, Lancet 389 (10066) (2017) 255–265, https://doi.org/10.1016/S0140-6736(16)32517-X.
[29] Edward B. Garon, Naiyer A. Rizvi, Rina Hui, Natasha Leighl, Ani S. Balmanoukian, Joseph Paul Eder, Amita Patnaik, Charu Aggarwal, Matthew Gubens, Leora Horn, Enric Carcereny, Myung-Ju Ahn, Enriqueta Felip, Jong-Seok Lee, Matthew D. Hellmann, Omid Hamid, Jonathan W. Goldman, Jean-Charles Soria, Marisa Dolled-Filhart, Ruth Z. Rutledge, Jin Zhang, Jared K. Lunceford, Reshma Rangwala, Gregory M. Lubiniecki, Charlotte Roach, Kenneth Emancipator, Leena Gandhi, Pembrolizumab for the Treatment of Non–Small-Cell Lung Cancer, N. Engl. J. Med. 372 (21) (2015) 2018–2028, https://doi.org/10.1056/NEJMoa1501824.
[30] N.A. Rizvi, J.R. Brahmer, S.-H.I. Ou, N.H. Segal, S. Khleif, W.-J.H. Gutierrez, P. Schoffski, O. Hamid, J. Weiss, J. Lutzky, M. Maio, J.J. Nemunaitis, D. Jaeger, A.S. Balmanoukian, M. Rebelatto, K. Steele, X. Li, J.A. Blake-Haskins, S.J. Antonia, Safety and clinical activity of MEDI4736, an anti-programmed cell death-ligand 1 (PD-L1) antibody, in patients with non-small cell lung cancer (NSCLC), J. Clin. Oncol. 33 (2015) 8032–8032.
[31] Julie Brahmer, Karen L. Reckamp, Paul Baas, Lucio Crinò, Wilfried E.E. Eberhardt, Elena Poddubskaya, Scott Antonia, Adam Pluzanski, Everett E. Vokes, Esther Holgado, David Waterhouse, Neal Ready, Justin Gainor, Osvaldo Arén Frontera, Libor Havel, Martin Steins, Marina C. Garassino, Joachim G. Aerts, Manuel Domine, Luis Paz-Ares, Martin Reck, Christine Baudelet, Christopher T. Harbison, Brian Lestini, David R. Spigel, Nivolumab versus Docetaxel in Advanced Squamous-Cell Non–Small-Cell Lung Cancer, N. Engl. J. Med. 373 (2) (2015) 123–135, https://doi.org/10.1056/NEJMoa1504627.
[32] R.S. Herbst, J. Soria, M. Kowanetz, G.D. Fine, O. Hamid, H.E.K. Kohrt, L. Horn, D. P. Lawrence, S. Rost, D.N.A. Way, S.S. Francisco, W.K. Ave, N. Carolina, Predictive correlates of response to the anti-PD-L1 antibody MPDL3280A, Nature 27 (2014) 563–567, https://doi.org/10.1038/nature14011.Predictive.
[33] National Cancer Institute, National Cancer Institute SEER Cancer Statistics Review 1975-2010, 2013. http://seer.cancer.gov/csr/1975_2012/.
[34] C. Allemani, H.K. Weir, H. Carreira, R. Harewood, D. Spika, X.S. Wang, F. Bannon, J. V. Ahn, C.J. Johnson, A. Bonaventure, R. Marcos-Gragera, C. Stiller, G. Azevedo E Silva, W.Q. Chen, O.J. Ogunbiyi, B. Rachet, M.J. Soeberg, H. You, T. Matsuda, M. Bielska-Lasota, H. Storm, T.C. Tucker, M.P. Coleman, Global surveillance of cancer survival 1995-2009: Analysis of individual data for 25 676 887 patients from 279 population-based registries in 67 countries (CONCORD-2), Lancet 385 (2015) 977–1010. https://doi.org/10.1016/S0140-6736(14)62038-9.
[35] Fabio Arnesano, Lucia Banci, Ivano Bertini, Isabella C. Felli, Maurizio Losacco, Giovanni Natile, Probing the interaction of cisplatin with the human copper chaperone atox1 by solution and in-cell NMR spectroscopy, J. Am. Chem. Soc. 133 (45) (2011) 18361–18369, https://doi.org/10.1021/ja207346p.
[36] P.R. dos Santos, M.R. Ely, F. Dumas, S. Moura, Synthesis, structural characterization and previous cytotoxicity assay of Zn(II) complex containing 1,10-phenanthroline and 2,2′-bipyridine with valproic acid, Polyhedron 90 (2015) 239–244, https://doi.org/10.1016/j.poly.2015.02.012.
[37] Maité Sylla-Iyarreta Veitía, Françoise Dumas, Georges Morgant, John R. J. Sorenson, Yves Frapart, Alain Tomas, Synthesis, structural analysis and anticonvulsant activity of a ternary Cu(II) mononuclear complex containing 1,10-phenanthroline and the leading antiepileptic drug valproic acid, Biochimie 91 (10) (2009) 1286–1293, https://doi.org/10.1016/j.biochi.2009.06.015.
[38] Mehmet Varol, Ayse Tansu Koparal, Kadriye Benkli, Rakibe Beklem Bostancioglu, Anti-lung Cancer and Anti-angiogenic Activities of New Designed Boronated Phenylalanine Metal Complexes, Curr Drug Deliv. 15 (10) (2018) 1417–1425, https://doi.org/10.2174/1567201815666180727145724.
[39] S. Parveen, F. Arjmand, S. Tabassum, Development and future prospects of selective organometallic compounds as anticancer drug candidates exhibiting novel modes of action, Eur. J. Med. Chem. 175 (2019) 269–286, https://doi.org/10.1016/j.ejmech.2019.04.062.
[40] Adrian Szczepaniak, Jakub Fichna, Organometallic compounds and metal complexes in current and future treatments of inflammatory bowel disease and colorectal cancer-a critical review, Biomolecules 9 (9) (2019) 398, https://doi.org/10.3390/biom9090398.
[41] Mehvash Zaki, Suboot Hairat, Elham S. Aazam, Scope of organometallic compounds based on transition metal-arene systems as anticancer agents: Starting from the classical paradigm to targeting multiple strategies, Royal Soc. Chem. 9 (6) (2019) 3239–3278, https://doi.org/10.1039/C8RA07926A.
[42] A. Latif Abuhijleh, Hijazi Abu Ali, Abdul-Hamid Emwas, Synthesis, spectral and structural characterization of dinuclear rhodium (II) complexes of the anticonvulsant drug valproate with theophylline and caffeine, J. Organomet. Chem. 694 (22) (2009) 3590–3596, https://doi.org/10.1016/j.jorganchem.2009.07.031.
[43] George M. Sheldrick, A short history of SHELX, Acta Crystallogr. Sect. A Found. Crystallogr. 64 (1) (2008) 112–122, https://doi.org/10.1107/S0108767307043930.
[44] F. Denizot, R. Lang, Rapid colorimetric assay for cell growth and survival. Modifications to the tetrazolium dye procedure giving improved sensitivity and reliability, J. Immunol. Methods 89 (1986) 271–277. http://www.ncbi.nlm.nih.gov/pubmed/3486233.
[45] H. Abu, M.D. Darawsheh, E. Rappocciolo, H. Abu Ali, M.D. Darawsheh, E. Rappocciolo, H. Abu, M.D. Darawsheh, E. Rappocciolo, A.A. Hijazi, Synthesis, crystal structure, spectroscopic and biological properties of mixed ligand complexes of zinc (II) valproate with 1, 10-phenanthroline and 2-aminomethylpyridine, Polyhedron 61 (2013) 235–241, https://doi.org/10.1016/j.poly.2013.06.015.
[46] M.C.S. Wong, X.Q. Lao, K.F. Ho, W.B. Goggins, S.L.A. Tse, Incidence and mortality of lung cancer: Global trends and association with socioeconomic status, Sci. Rep. 7 (2017) 1–9, https://doi.org/10.1038/s41598-017-14513-7.
[47] K. Drott, H. Hagberg, K. Papworth, T. Relander, M. Jerkeman, Valproate in combination with rituximab and CHOP as first-line therapy in diffuse large B-cell lymphoma (VALFRID), Blood Adv. 2 (2018) 1386–1392, https://doi.org/10.1182/bloodadvances.2018019240.
[48] Jose Ramiro Espinoza-Zamora, Juan Labardini-Méndez, Alejandro Sosa-Espinoza, Celia López-González, Magnolia Vieyra-García, Myrna Candelaria, Valentin Lozano-Zavaleta, Diana Vanesa Toledano-Cuevas, Nidia Zapata-Canto, Eduardo Cervera, Alfonso Dueñas-González, Efficacy of hydralazine and valproate in cutaneous T-cell lymphoma, a phase II study, Expert Opin. Investig. Drugs. 26 (4) (2017) 481–487, https://doi.org/10.1080/13543784.2017.1291630.
[49] M. Candelaria, D. Gallardo-Rincón, C. Arce, L. Cetina, J.L. Aguilar-Ponce, Ó Arrieta, A. González-Fierro, A. Chávez-Blanco, E. de la Cruz-Hernández, M. F. Camargo, C. Trejo-Becerril, E. Pérez-Cárdenas, C. Pérez-Plasencia, L. Taja-Chayeb, T. Wegman-Ostrosky, A. Revilla-Vazquez, A. Dueñas-González, A phase II study of epigenetic therapy with hydralazine and magnesium valproate to overcome chemotherapy resistance in refractory solid tumors, Ann. Oncol. 18 (9) (2007) 1529–1538, https://doi.org/10.1093/annonc/mdm204.
[50] Alfonso Duenas-Gonzalez, Myrna Candelaria, Carlos Perez-Plascencia, Enrique Perez-Cardenas, Erick de la Cruz-Hernandez, Luis A. Herrera, Valproic acid as epigenetic cancer drug: Preclinical, clinical and transcriptional effects on solid tumors, Cancer Treat. Rev. 34 (3) (2008) 206–222, https://doi.org/10.1016/j.ctrv.2007.11.003.
[51] Alfonso Dueñas-Gonzalez, Jaime Coronel, Lucely Cetina, Aurora González-Fierro, Alma Chavez-Blanco, Lucia Taja-Chayeb, Hydralazine-valproate: A repositioned drug combination for the epigenetic therapy of cancer, Expert Opin. Drug Metab. Toxicol. 10 (10) (2014) 1433–1444, https://doi.org/10.1517/17425255.2014.947263.
[52] Yang Hao, Guodong Wang, Chao Lin, Dong Li, Zhonghao Ji, Fei Gao, Zhanjun Li, Dianfeng Liu, Dongxu Wang, Valproic Acid Induces Decreased Expression of H19 Promoting Cell Apoptosis in A549 Cells, DNA Cell Biol. 36 (6) (2017) 428–435, https://doi.org/10.1089/dna.2016.3542.